Fluid Dynamics &
Materials Processing

Tech Science Press

http://doi.org/10.32604/fdmp.2026.086018

ARTICLE

A Temperature-Pressure Coupled Model for Predicting Sand Production during Multi-Thermal Fluid Huff-and-Puff in Unconsolidated Sandstone Reservoirs

Zhuwei Tao, Yanfeng He*, Hui Xu*, Shengda Zhang, Zetao Sun, Ying Wu, Peng Li and Xing Shi

School of Petroleum and Natural Gas Engineering, Changzhou University, Changzhou, China
*Corresponding Authors: Yanfeng He. Email: heyanfeng@cczu.edu.cn; Hui Xu. Email: xuhui@cczu.edu.cn

Received: 22 May 2026; Accepted: 01 September 2026; Published: 04 September 2026

ABSTRACT: This study elucidates the mechanisms governing sand production during multi-thermal fluid huff-and-puff in unconsolidated sandstone heavy oil reservoirs and develops a temperature-pressure coupled prediction model for accurately quantifying sand production. Orthogonal laboratory experiments were conducted on reservoir samples from a representative case (Block X, Oilfield L), to compare the mechanical response and sand production behavior under multi-thermal fluid and conventional steam stimulation. The relative importance of the governing parameters was quantified using analysis of variance (ANOVA), and an exponential prediction model incorporating the coupled effects of temperature and pressure was established. The results reveal that temperature and pressure are the primary factors controlling both rock stiffness degradation and sand production, with highly significant statistical effects. Compared with conventional steam injection, multi-thermal fluid stimulation induces more pronounced rock weakening and substantially greater sand production owing to the combined effects of CO_2 dissolution and N_2 gas channelling. It also generates coarser produced particles and promotes wormhole formation. The optimum operating conditions were identified as an injection temperature of 130°C, a pressure of 10 MPa, a CO_2/N_2 volume ratio of 0.5, and an injection volume of 10 mL. The proposed model reproduces the experimental observations with excellent accuracy, achieving a coefficient of determination exceeding 0.98 and consistently outperforming conventional single-variable prediction models.

KEYWORDS: Multi-thermal fluid; heavy oil reservoir; orthogonal experiment; sand production; prediction model

1 Introduction

Heavy oil resources are widely distributed and constitute a substantial component of global petroleum resources. However, heavy oils typically have high viscosities, high resin and asphaltene contents, and occur in strongly heterogeneous reservoirs, making their development challenging. Heavy oil production currently relies mainly on thermal recovery technologies, including cyclic steam stimulation (CSS), steam flooding, and steam-assisted gravity drainage (SAGD). These methods raise reservoir temperature and reduce crude-oil viscosity by injecting high-temperature steam into the formation, thereby mobilizing and producing heavy oil [1]. However, as heavy oil development extends to deeper, thinner, lower-permeability, and more heterogeneous reservoirs, conventional steam-based thermal recovery faces increasingly serious limitations. First, substantial heat is lost as steam travels through the wellbore and reservoir. Because of steam override and gravity segregation, heat is distributed nonuniformly within the target interval, reducing thermal efficiency and dissipating energy into surrounding rock and non-target zones. Second, steam

Copyright © 2026 The Authors. Published by Tech Science Press. This work is licensed under a Creative Commons Attribution 4.0 International License, which permits unrestricted use, distribution, and reproduction in any medium, provided the original work is properly cited.

stimulation primarily reduces viscosity through heating but has limited ability to disrupt the aggregated macromolecular structures of resins and asphaltenes. During later production stages, steam-channeling and steam-breakthrough pathways readily develop, causing nonuniform vertical and areal sweep, a continuing decline in the oil–steam ratio, and progressively poorer development performance [2].

To overcome the technical limitations of conventional steam-based thermal recovery, synergistic recovery technologies based on multicomponent thermal fluids have attracted increasing attention. Compared with conventional steam flooding, multicomponent thermal-fluid systems combine thermal effects, dissolution-induced viscosity reduction, and enhanced displacement mechanisms [3–6]. Steam rapidly increases reservoir temperature and lowers crude-oil viscosity. CO_2 dissolves in heavy oil, causing oil swelling, reducing interfacial tension, and weakening intermolecular interactions among resin and asphaltene molecules, thereby further improving crude-oil mobility [7]. Meanwhile, N_2 supplements reservoir energy, enlarges the swept volume, and mitigates steam override [8]. The combined action of these mechanisms can improve thermal utilization efficiency, expand the steam-swept area, and increase oil recovery. Accordingly, multicomponent thermal-fluid technology is considered an important option for improving late-stage cyclic steam stimulation and recovering difficult-to-produce heavy oil reserves. However, while multicomponent thermal fluids improve displacement efficiency, they also alter reservoir stress conditions and fluid-flow characteristics. The coupled effects of high temperature, high pressure, and multiphase flow can further weaken the reservoir framework and promote particle migration, thereby increasing the risk of sand production. Severe sand production not only reduces well productivity but can also block the wellbore, erode surface equipment, and shorten well service life; it is therefore a major constraint on the large-scale application of multicomponent thermal-fluid technologies [9]. Investigating sand-production patterns and mechanisms under multicomponent thermal-fluid conditions is therefore essential for the safe and efficient development of heavy oil reservoirs.

Extensive studies worldwide have addressed sand production during the development of conventional sandstone oil and gas reservoirs through theoretical modeling, numerical simulation, and laboratory experimentation. Existing theoretical models primarily establish relationships between near-wellbore rock instability and sand production using rock-strength criteria [10,11]. Numerical approaches dynamically predict the initiation and evolution of sand production by coupling geomechanical stress fields with fluid-flow fields [12–14]. Laboratory physical-simulation experiments provide essential observations for validating these models and calibrating their parameters. Previous studies have shown that temperature [15], pressure [16], fluid composition [17], flow rate [18], injection volume [19], and reservoir cementation [20] can significantly affect sand-production behavior. These investigations have clarified the controlling effects of individual factors and have supported the development of corresponding prediction methods. However, most studies have focused on conventional sandstone reservoirs and have considered either a single factor, such as temperature or pressure, or a single rock-strength criterion. Consequently, interactions among temperature, pressure, fluid composition, and flow conditions are not adequately represented in many existing approaches. Systematic studies of these coupled mechanisms remain limited. In particular, under multicomponent thermal-fluid development conditions, individual components can simultaneously alter rock chemistry, stress, and multiphase flow. Their effects on reservoir-rock mechanical properties and on the time-dependent evolution of sand production have not yet been fully clarified.

Based on these considerations, this study investigates an unconsolidated sandstone heavy-oil reservoir from Block X in the L Oilfield. Laboratory simulation experiments were conducted to characterize changes in reservoir-rock mechanical properties and the dynamic evolution of sand production over repeated multicomponent thermal-fluid huff-and-puff cycles. By combining an orthogonal experimental design with

analysis of variance (ANOVA), the effects of temperature, pressure, CO_2/N_2 volume ratio, and injection volume on elastic modulus and sand-production behavior were systematically evaluated. The relative influence and statistical significance of each factor were analyzed, and the dominant controlling factors were identified. Unlike conventional prediction methods based on a single factor or a single strength criterion, the proposed approach explicitly incorporates multicomponent thermal-fluid operating conditions and composition into the sand-production evaluation framework. Separate exponential relationships were first developed for temperature and pressure, after which a coupled pressure–temperature sand-production model was established to quantify reservoir sand-production risk under complex thermal-fluid conditions. The findings provide a theoretical basis and technical support for sand-production risk control, production optimization, and injection–production parameter design during multicomponent thermal-fluid operations in the study block. The results also provide a reference for the safe and efficient development of similar unconsolidated sandstone heavy oil reservoirs.

2 Sand Production Experiments

2.1 Reservoir Characteristics of Block X in the L Oilfield

Block X in the L Oilfield is a typical unconsolidated sandstone heavy oil reservoir buried at a depth of 320–580 m. The reservoir is characterized by high porosity and high permeability. The original reservoir temperature is approximately 50°C, and the initial formation pressure ranges from 5 to 15 MPa. The overburden stress and minimum horizontal principal stress are 7.2–12.5 MPa and 5.1–8.9 MPa, respectively.

The main producing interval has a porosity of 28%–36% and a permeability of 500–1500 mD. The reservoir rock consists predominantly of unconsolidated sandstone, with grain sizes of 5–800 μm and a relatively high proportion of fine particles. X-ray diffraction (XRD) analysis indicates that the mineral assemblage consists mainly of quartz, feldspar, clay minerals, and carbonate cements. Weak cementation and abundant fine-grained particles make the reservoir highly susceptible to sand production during thermal recovery.

The initial oil saturation ranges from 58% to 72%. At the original reservoir temperature of 50°C, the dead-oil viscosity is 4100–7900 mPa·s, resulting in poor fluid mobility and limiting the effectiveness of conventional production methods. Block X in the L Oilfield therefore provides an appropriate geological setting for investigating sand-production mechanisms during multicomponent thermal-fluid huff-and-puff and for developing a coupled thermo-hydro-chemical-mechanical sand-production model.

2.2 Experimental Methods

An orthogonal experimental design uses a balanced subset of factor-level combinations from the corresponding full factorial design, thereby reducing the experimental burden while retaining efficient estimates of the main effects. Within an orthogonal array, each factor level occurs equally often and in balanced combinations with the levels of the other factors, enabling efficient comparison of factor effects. This approach can provide substantial information with relatively few experiments, thereby reducing time and cost.

2.3 Experimental Apparatus

The experiments were conducted using a purpose-built apparatus designed to simulate sand production during multicomponent thermal-fluid stimulation of heavy oil reservoirs. The apparatus enables direct visualization of fluid and particle outflow during displacement. A schematic of the setup is shown in Fig. 1.

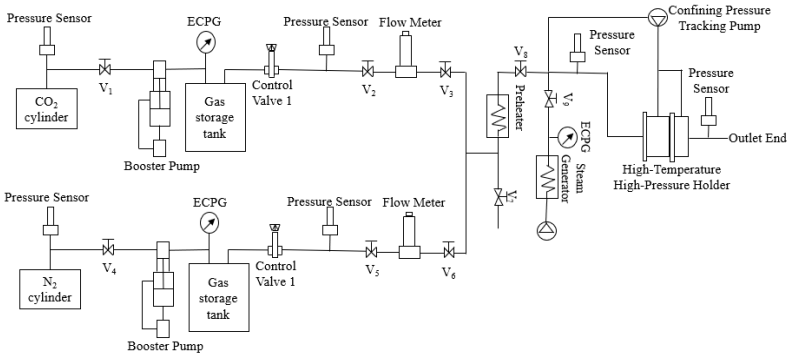

Figure 1: Experimental apparatus for simulating heavy-oil huff-and-puff with a multicomponent thermal fluid.

(1) The CO_2 and N_2 booster pumps compress gas from the respective cylinders to provide the required inlet pressure.
(2) The steam generator produces high-temperature steam, and the preheater further heats the mixed fluid to reproduce the downhole thermal environment.
(3) The high-temperature, high-pressure holder secures the core sample. After core permeability is measured, the sample is placed in the holder. Confining pressure is applied to simulate *in situ* formation pressure, and the core is heated to the target formation temperature. After the pressure difference between the inlet and outlet is established, the multicomponent thermal fluid (CO_2/N_2/steam) is injected into the holder. Pressure sensors at key locations monitor system pressure in real time, while flow meters independently control the CO_2 and N_2 injection rates.

2.4 Experimental Design

A well-designed experimental program controls all target parameters within specified ranges so that factor effects can be evaluated systematically and efficiently. On the basis of conditions in Block X, an orthogonal experimental design was adopted to reduce the required number of tests while retaining balanced comparisons among factor levels. Four factors—temperature, pressure, injection volume, and CO_2/N_2 volume ratio—were selected. A four-level design comprising 16 tests was used to evaluate the effects of these factors on the response variables. The factors and their corresponding levels are listed in Table 1.

Table 1: Values of the independent variables used in the experimental design.

Factor	Unit	Orthogonal Experimental Design for Multicomponent Thermal-Fluid Huff-and-Puff				Orthogonal Experimental Design for Steam Huff-and-Puff			
		Levels				Levels			
		1	2	3	4	1	2	3	4
A: Temperature	°C	80	105	130	155	80	105	130	155
B: Pressure	MPa	6	8	10	12	6	8	10	12
C: Injection volume	mL	5	10	15	20	5	10	15	20
D: CO_2/N_2 volume ratio		0.33	0.50	0.66	0.83				

The experiments were performed using a purpose-built multicomponent thermal-fluid huff-and-puff sand-production simulation system that permits direct visualization of the cyclic stimulation process. The system has a maximum fluid flow rate of 66 mL/min, a maximum confining pressure of 25 MPa, and

a maximum core-holder temperature of 250°C. The particle-size distribution of the produced sand was measured with a laser particle-size analyzer, while mechanical properties, including elastic modulus and Poisson's ratio, were evaluated using an acoustic-mechanical test system.

3 Results and Analysis

The sand-production simulation comprised five huff-and-puff cycles, with a soaking period of 30 min in each cycle. The experimental results for the 16 multicomponent thermal-fluid tests and the 16 steam huff-and-puff tests are presented in Figs. 2 and 3.

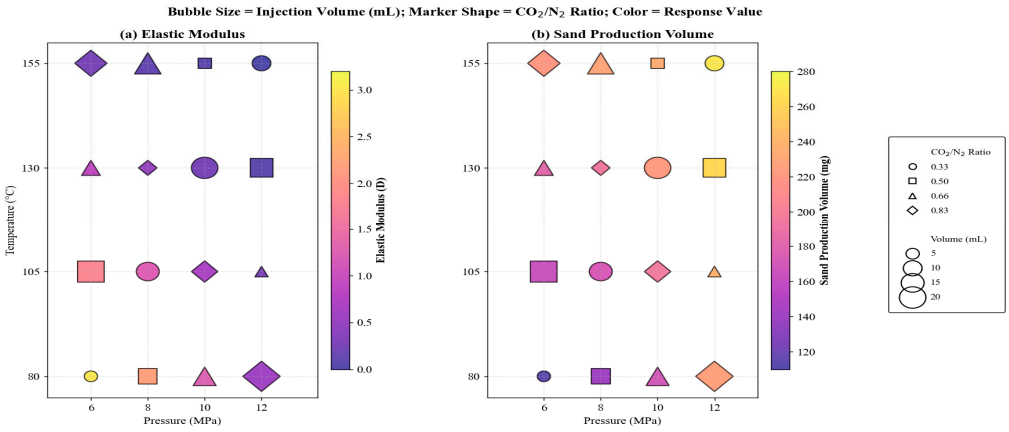

Figure 2: Elastic modulus (**a**) and sand-production (**b**) results for multicomponent thermal-fluid huff-and-puff.

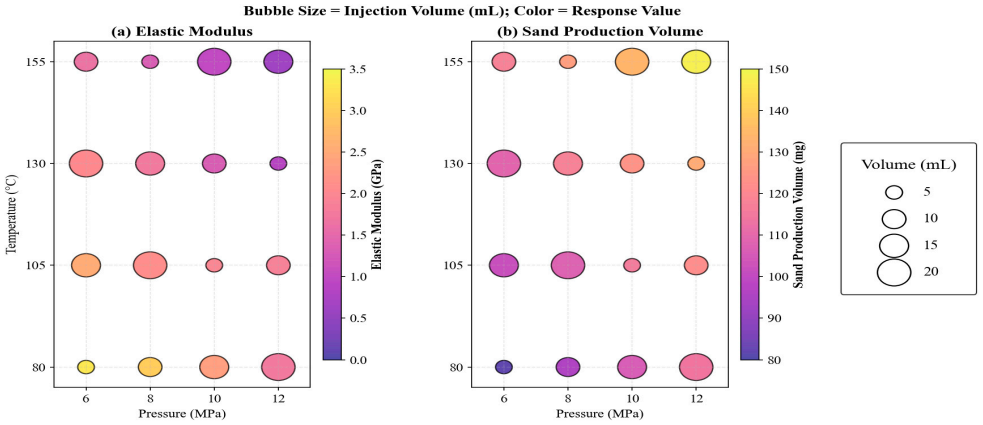

Figure 3: Elastic modulus (**a**) and sand-production (**b**) results for steam huff-and-puff.

Figs. 2 and 3 each contain two panels: (a) elastic modulus and (b) produced-sand mass. The horizontal axis represents injection pressure (MPa), and the vertical axis represents formation temperature (°C). In Fig. 2, marker shape identifies the CO_2/N_2 volume ratio: circles, squares, triangles, and diamonds correspond to 0.33, 0.50, 0.66, and 0.83, respectively. In both figures, marker size represents injection volume (mL), with larger markers indicating larger volumes. Marker color indicates the response value; bright yellow denotes high values and dark blue denotes low values. The figures therefore summarize the combined effects of pressure, temperature, CO_2/N_2 volume ratio, and injection volume on elastic modulus and sand production.

3.1 Comparative Mechanical Analysis of Multicomponent Thermal-Fluid and Steam Huff-and-Puff Treatments

Analysis of variance (ANOVA) was used to evaluate the main effects and their statistical significance. The F-value is the ratio of the factor mean square to the residual mean square, while the *p*-value indicates whether the observed factor effect is statistically significant at the selected significance level.

The ANOVA results in Tables 2 and 3 show broadly similar effects of temperature and pressure on reservoir-rock elastic modulus under multicomponent thermal-fluid and steam huff-and-puff conditions. For the multicomponent thermal-fluid experiments, the factor ranking based on F-values was temperature > pressure > CO_2/N_2 volume ratio > injection volume. The F-values for temperature and pressure were 32.222 and 18.227, respectively, with corresponding *p*-values of 0.0088 and 0.0198; both effects were significant at the 0.05 level. The CO_2/N_2 volume ratio had an F-value of 5.587 and a *p*-value of 0.0957, whereas injection volume had an F-value of 1.253 and a *p*-value of 0.4287. Thus, neither of these latter effects was statistically significant at the 95% confidence level, although the gas ratio showed a stronger numerical influence than injection volume. For steam huff-and-puff, temperature and pressure were also significant, with F-values of 38.050 and 20.087 and *p*-values of 0.0069 and 0.0173, respectively. Injection volume had an F-value of 1.422 and a *p*-value of 0.3896 and therefore exerted a comparatively limited direct effect. Overall, temperature was the primary factor affecting reservoir-rock mechanical properties, followed by pressure. Mean elastic modulus generally decreased as temperature, pressure, injection volume, and CO_2/N_2 volume ratio increased, indicating progressive weakening of the rock framework; however, the effects of injection volume and gas ratio were not statistically significant.

Table 2: ANOVA of elastic modulus in the multicomponent thermal-fluid orthogonal experiments.

Factor	Sum of Squares	Degrees of Freedom	F-Value	*p*-Value	Significance
A	6.419	3	32.222	0.0088	Significant
B	3.631	3	18.227	0.0198	Significant
C	0.249	3	1.253	0.4287	-
D	1.113	3	5.587	0.0957	-
Error	0.199	3	-		-
Total	11.611	15	-		-

Table 3: ANOVA of elastic modulus in the steam huff-and-puff orthogonal experiments.

Factor	Sum of Squares	Degrees of Freedom	F-Value	*p*-Value	Significance
A	5.027	3	38.050	0.0069	Significant
B	2.653	3	20.087	0.0173	Significant
C	0.187	3	1.422	0.3896	-
Error	0.132	3	-		-
Total	7.999	15	-		-

Under identical temperature, pressure, and injection-volume conditions, multicomponent thermal-fluid stimulation had a stronger effect on the mechanical properties of heavy-oil reservoir rocks than steam stimulation. This difference is attributable to the combined thermal, chemical, and hydrodynamic effects of the multicomponent thermal-fluid system.

First, dissolved CO_2 reacts with carbonate minerals and cementing materials in the reservoir rock, causing mineral dissolution, weakening intergranular cementation, and enlarging pore space. These processes can improve permeability and fluid-flow capacity but also reduce the mechanical integrity of the rock

framework. For example, Guo [21] reported that increasing temperature and pressure intensified the dissolution of clay minerals, mainly illite and montmorillonite, promoted framework-particle detachment and migration, and amplified pore-structure evolution during CO_2-assisted multicomponent thermal-fluid injection. The resulting coupled thermal–hydrological–geochemical processes increased porosity–permeability fluctuations and the susceptibility of unconsolidated sandstone to sand production. These observations support the mechanism by which high-temperature, CO_2-rich fluids weaken the rock framework through mineral dissolution and particle migration.

Second, N_2 promotes gas channeling and preferential flow. Owing to its high diffusivity and mobility, N_2 can readily enter connected pore networks and microfractures, alter local stress distributions, and facilitate particle detachment and migration [22]. This process enhances reservoir connectivity, supplements formation energy, and can contribute to improved heavy-oil recovery. Steam alone has a much weaker gas-channeling effect and therefore exerts a less pronounced hydrodynamic influence on rock mechanical behavior. Fu [23] investigated N_2-foam-assisted steam flooding and reported that, during conventional steam injection, steam preferentially propagated through high-permeability pathways because of reservoir heterogeneity, causing early breakthrough and limited sweep efficiency. Adding N_2 changed the mobility ratio and flow-field distribution, allowing the injected gas to enter dominant flow channels and reshape fluid-migration pathways. The resulting redistribution of the displacement front altered the spatial distribution of residual oil and intensified local seepage velocities. In a weakly cemented reservoir, these concentrated flow paths can impose greater drag and pressure-gradient forces on sandstone grains. The grains may then detach from cementing contacts, migrate through enlarged pores or wormholes, and be transported to the production outlet. These observations provide a physical basis for the proposed N_2-channeling mechanism and its contribution to enhanced particle migration and sand production.

Multicomponent thermal-fluid injection can therefore improve reservoir permeability, connectivity, and heavy-oil recovery. However, thermal weakening, CO_2-induced mineral dissolution, and N_2-induced hydrodynamic erosion collectively reduce the stability of the rock framework and increase particle detachment and transport, thereby elevating sand-production risk.

3.2 Comparative Analysis of Sand Production during Multicomponent Thermal-Fluid and Steam Huff-and-Puff

3.2.1 Observed Phenomena during Multicomponent Thermal-Fluid and Steam Huff-and-Puff

Each sand-production test comprised five huff-and-puff cycles, with a soaking period of 30 min per cycle.

Compared with steam huff-and-puff, the fluid produced after the first soaking period of multicomponent thermal-fluid huff-and-puff was an oil–water mixture with a relatively high oil yield and abundant fine sand. Steam huff-and-puff yielded a moderate amount of oil, lower than that obtained with the multicomponent thermal fluid, and produced less sand. Fig. 4a,b shows the oil- and sand-production observations for the multicomponent thermal-fluid cycle, whereas Fig. 4c,d shows the corresponding observations for steam huff-and-puff.

As shown in Fig. 5, the particle-size distribution of produced sand differed markedly between steam and multicomponent thermal-fluid huff-and-puff. Under steam stimulation, the median particle size (d_{50}) was approximately 100 μm, and most particles were distributed within 10–200 μm. The produced material consisted predominantly of fine grains. This pattern indicates that steam caused comparatively limited deterioration of the rock framework and primarily promoted the detachment and migration of fine particles from weak cementing contacts. Under multicomponent thermal-fluid stimulation, the median particle

size increased to approximately 200 μm, and most particles ranged from approximately 10 to 400 μm. A noticeable fraction of coarse particles measuring 200–800 μm was also observed. Thus, relative to steam stimulation, the multicomponent thermal-fluid system produced sand with a substantially larger median size, a broader size distribution, and greater particle-size variability. The mobilization of coarser grains suggests that damage extended beyond the release of fines and involved degradation of the load-bearing rock framework. These results are consistent with more intense grain detachment, weakening of intergranular cementation, enlargement of connected channels, and local framework failure, all of which allow larger formation particles to migrate and be produced.

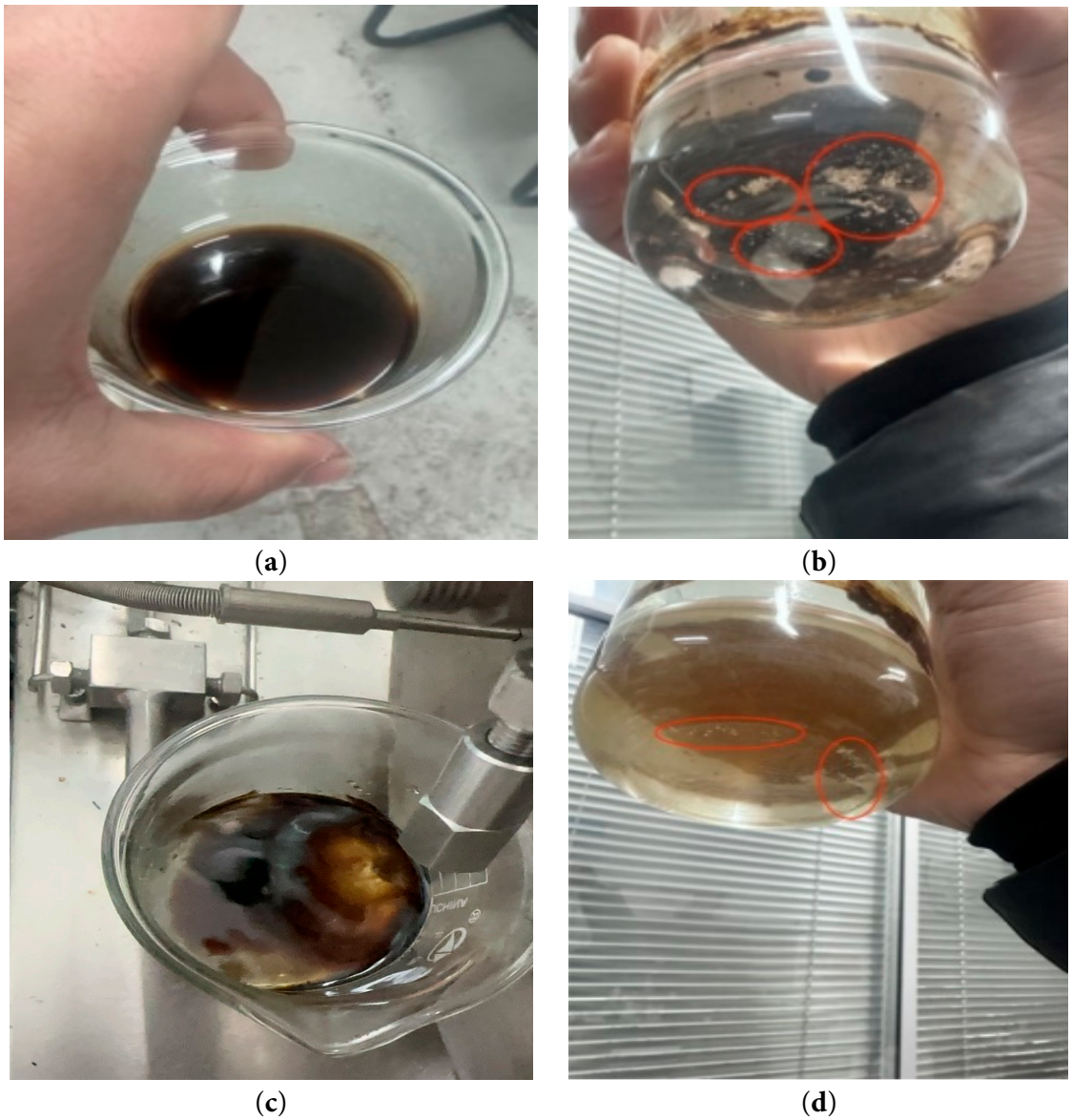

Figure 4: Oil and sand production. (**a**) Oil produced during one multicomponent thermal-fluid huff-and-puff cycle; (**b**) sand produced during one multicomponent thermal-fluid huff-and-puff cycle; (**c**) oil produced during steam huff-and-puff; and (**d**) sand produced during steam huff-and-puff.

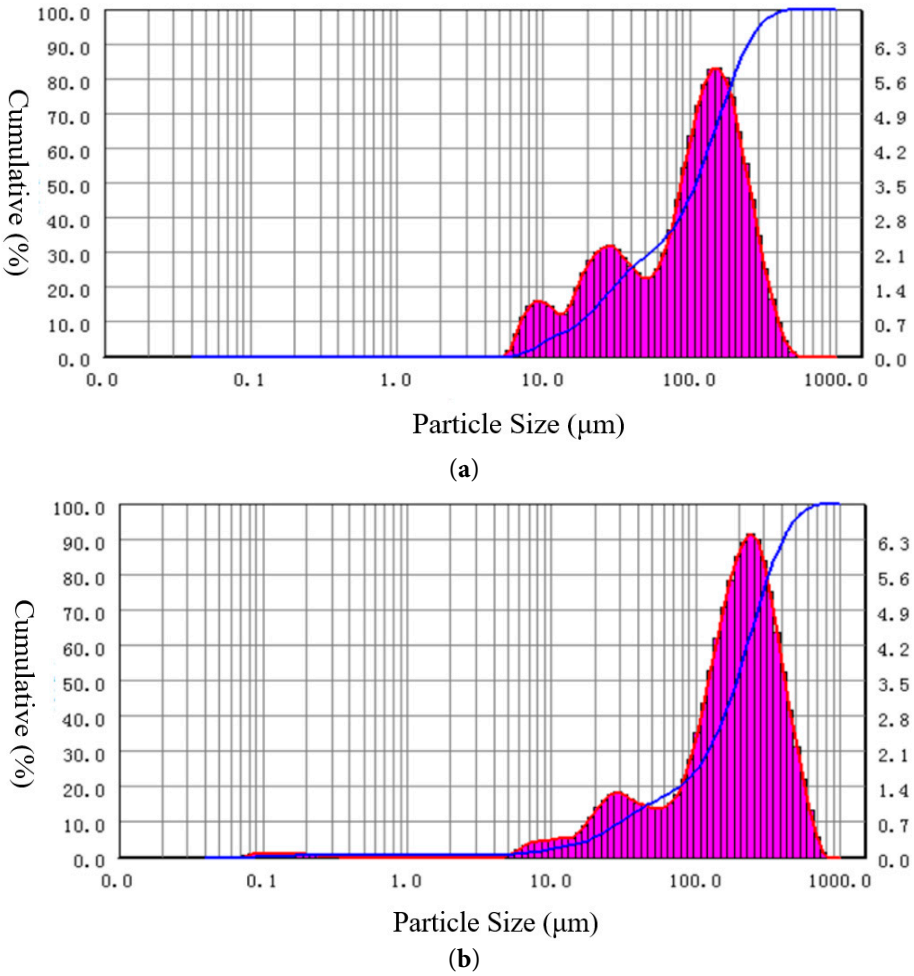

Figure 5: Particle-size distributions of sand produced during steam and multicomponent thermal-fluid huff-and-puff. (**a**) Steam huff-and-puff; (**b**) multicomponent thermal-fluid huff-and-puff.

When the system was opened to production after multicomponent thermal-fluid soaking, gas channeling occurred at a reservoir pressure of approximately 3 MPa and was accompanied by violent sand-and-gravel ejection and a distinct hissing sound. Gas channeling occurred mainly during the interval without oil production. After channeling ceased, oil production resumed in most tests; however, because formation energy and production pressure were insufficient, the heavy oil flowed slowly and could not be fully recovered. Gas channeling also occurred at approximately 3 MPa after steam huff-and-puff, but it was much weaker than that observed after multicomponent thermal-fluid huff-and-puff.

After multicomponent thermal-fluid huff-and-puff, well-developed wormholes with wide openings formed on the core sidewall within the red-circled area, with a visible surface length of approximately 1.7 cm. Interconnected pores were observed inside the wormholes, and the surrounding rock matrix was loose and fragmented. The channels extended deep into the core, and numerous sand grains spalled from the pore walls, indicating substantial alteration of the rock framework by CO_2 dissolution and gas erosion. By contrast, the steam-treated core showed only a narrow, fissure-like wormhole with a surface length of approximately 1.2 cm in the red-circled area on the axial end face. This channel had a small aperture and limited extent and caused only minor damage to the core framework.

Comparison of the two cores indicates that CO_2 dissolution and high-pressure N_2 erosion in the multicomponent thermal-fluid system generated wide, deep wormholes after only three huff-and-puff cycles. These wormholes acted as high-conductivity channels for gas flow and coarse-particle production. Steam, by contrast, altered the rock primarily through thermal effects. Wormholes were not observed until the fifth steam huff-and-puff cycle, and the resulting channels were narrow and short. Accordingly, steam caused less damage to the rock framework and a lower sand-production risk than multicomponent thermal-fluid huff-and-puff, as shown in Fig. 6.

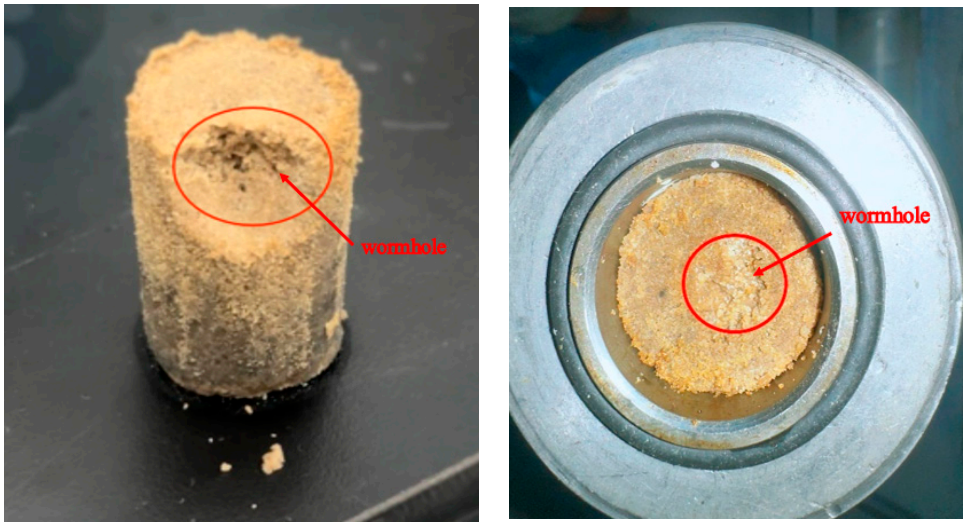

(**a**) (**b**)

Figure 6: Wormholes formed during multicomponent thermal-fluid and steam huff-and-puff. (**a**) Wormholes after multicomponent thermal-fluid stimulation; (**b**) wormholes after steam huff-and-puff.

3.2.2 Comparison of Sand-Production Results for Multicomponent Thermal-Fluid and Steam Huff-and-Puff

Tables 4 and 5 present the ANOVA results for sand production under multicomponent thermal-fluid and steam huff-and-puff conditions, respectively. Temperature and pressure were the dominant factors for both recovery methods. In the steam experiments, temperature and pressure had F-values of 93.98 and 62.17 and *p*-values of 0.0000196 and 0.0000654, respectively. The F-value ranking was temperature > pressure > injection volume, indicating that thermal weakening was the primary driver of increased sand production. In the multicomponent thermal-fluid experiments, pressure and temperature had F-values of 168.98 and 144.30 and *p*-values of 0.00076 and 0.00097, respectively. Both effects were statistically significant at the 1% level. The ranking based on Table 4 was pressure > temperature > injection volume > CO_2/N_2 volume ratio. Injection volume and CO_2/N_2 volume ratio had *p*-values of 0.07321 and 0.09081, respectively, and were therefore not significant at the 0.05 level. Compared with steam stimulation, the additional chemical dissolution caused by CO_2 and the channelized gas flow promoted by N_2 further damaged the rock framework, facilitated particle migration, and increased overall sand production.

As shown in Table 6, the range for pressure was 80.5 and that for temperature was 76, confirming that these two variables exerted the strongest effects on sand production. The ranges for CO_2/N_2 volume ratio and injection volume were both 15.25, indicating comparatively small effects. Based on the mean sand-production response at each factor level and consideration of both rock-framework stability and development performance, the following operating combination was selected for multicomponent thermal-fluid huff-and-puff: 130°C, 10 MPa, a CO_2/N_2 volume ratio of 0.5, and an injection volume of 10 mL.

Table 4: ANOVA of produced-sand mass in the multicomponent thermal-fluid orthogonal experiments.

Factor	Sum of Squares	Degrees of Freedom	F-Value	*p*-Value	Significance
A	12,581.187	3	144.30	0.00097	Significant
B	14,733.187	3	168.98	0.00076	Significant
C	603.687	3	6.92	0.07321	-
D	508.687	3	5.83	0.09081	-
Error	87.187	3	-		-
Total	28,513.933	15	-		-

Table 5: ANOVA of produced-sand mass in the steam huff-and-puff orthogonal experiments.

Factor	Sum of Squares	Degrees of Freedom	F-Value	*p*-Value	Significance
A	2226.1875	3	93.98	0.0000196	Significant
B	1472.6875	3	62.17	0.0000654	Significant
C	24.6875	3	1.04	0.44005	-
Error	47.375	6	-		-
Total	3770.9375	15	-		-

Table 6: Range analysis of the multicomponent thermal-fluid orthogonal experiments.

	Temperature	Pressure	CO_2/N_2 Volume Ratio	Injection Volume
K1	163.00	169.50	195.75	194.50
K2	193.00	184.50	197.75	200.75
K3	215.25	206.25	205.75	205.25
K4	239.00	250.00	211.00	209.75
R	76.00	80.50	15.25	15.25

CO_2 in the multicomponent thermal fluid has a strong dissolution effect. After injection into the heavy-oil reservoir, dissolved CO_2 forms an acidic fluid that reacts with carbonate minerals and some cementing materials, thereby promoting mineral dissolution. This process can increase porosity and permeability, improve fluid connectivity, and facilitate heavy-oil flow. At the same time, dissolution weakens intergranular bonds and can detach rock particles, increasing sand-production potential. The micropores, enlarged pore throats, and fractures created or extended by dissolution provide connected pathways for sand-grain migration. Consequently, particles that were initially retained within the framework can be mobilized more readily during pressure release and production.

Second, N_2 promotes gas channeling during production. Because of its mobility, N_2 can rapidly enter microfractures, larger pores, and preferential flow paths, altering local pressure gradients, stress distributions, and the mechanical response of the rock. Gas channeling can improve reservoir connectivity, supplement formation energy, and enhance heavy-oil recovery by extending the effective displacement range. However, concentrated gas flow also increases local seepage velocity and hydrodynamic loading. The resulting stress redistribution and drag forces can loosen weakly cemented grains, enlarge existing channels, and increase the probability that detached particles will be transported to the wellbore.

Compared with conventional steam development, the multicomponent thermal-fluid process provides additional operational flexibility but does not inherently reduce sand production; the present experiments instead show greater rock-framework weakening and higher sand output. Steam development relies mainly on heat transfer and heavy-oil viscosity reduction, and its dissolution effect on reservoir rock is

comparatively weak. In the multicomponent thermal-fluid process, the CO_2/N_2 composition, injection volume, temperature, and pressure provide additional variables that can be adjusted to manage the tradeoff between recovery enhancement and sand-production risk. Reasonable parameter control may therefore limit, rather than eliminate, sand production while maintaining recovery performance and reservoir stability. A quantitative model suitable for multicomponent thermal-fluid huff-and-puff is needed to describe and predict sand production, clarify the relationships between the key operating variables and sand output, and support optimization of field injection and production parameters.

3.3 Sand-Production Model for Multicomponent Thermal-Fluid Huff-and-Puff

Temperature and pressure were identified as the two primary factors affecting reservoir sand production and rock mechanical properties during multicomponent thermal-fluid huff-and-puff. To quantify sand-production behavior in heavy-oil reservoirs, separate prediction models were first developed using temperature and pressure as the principal variables. The models were then compared on the basis of goodness of fit and agreement with the experimental data.

At a given pressure, sand production exhibited an exponential relationship with temperature. A temperature-based prediction model was therefore established as follows:

$$y = A + B\boldsymbol{e}^{CT} \tag{1}$$

where y is the sand production under laboratory conditions (mg);

T is the multicomponent thermal-fluid injection temperature (°C);

A, B and C are pressure-dependent coefficients.

The coefficients at different pressures are listed in Table 7. Coefficients A, B, and C were fitted as functions of injection pressure, and all three showed exponential relationships with pressure. The corresponding expressions are given in Eqs. (2)–(4), with coefficients of determination (R^2) of 0.98, 0.95, and 0.99, respectively. These relationships were incorporated into the temperature-based model so that both injection pressure and temperature were represented.

$$A = 705.29124\boldsymbol{e}^{-0.10056P} + 66.74651 \tag{2}$$

$$B = -1231.00106\boldsymbol{e}^{-0.22539P} - 188.5847 \tag{3}$$

$$C = -0.0000030262\boldsymbol{e}^{0.71287P} - 0.00493 \tag{4}$$

At a given temperature, sand production exhibited an exponential relationship with pressure. A pressure-based prediction model was therefore established as follows:

$$y = D + E\mathbf{e}^{FP} \tag{5}$$

where y is the sand production under laboratory conditions (mg);

P is the multicomponent thermal-fluid injection pressure (MPa);

D, E and F are temperature-dependent coefficients.

The coefficients at different temperatures are listed in Table 8. Coefficients D, E, and F were fitted as functions of temperature, and all three showed exponential relationships with temperature. The corre-

sponding expressions are given in Eqs. (6)–(8), with R^2 values of 0.99, 0.98, and 0.94, respectively. These relationships were incorporated into the pressure-based model so that both pressure and temperature were represented.

$$D = -629.5991\mathbf{e}^{-0.00513T} + 491.44758 \tag{6}$$

$$E = 34.63468\boldsymbol{e}^{-0.01025T} - 5.06554 \tag{7}$$

$$F = 1.69444\boldsymbol{e}^{0.0000415511T} - 1.52746 \tag{8}$$

Both models can be used to estimate laboratory sand production for specified pressure and temperature conditions. Comparison of the fitting curves showed that the temperature-based fits at different pressures generally had higher R^2 values, better goodness of fit, and closer agreement with the experimental data than the pressure-based fits. The reported correlation coefficient between predicted and experimental values was 0.99 for the temperature-based model and 0.98 for the pressure-based model. The temperature-based equation was therefore selected as the basis for the coupled pressure–temperature sand-production model for multicomponent thermal-fluid huff-and-puff. The model parameters were fitted using experiments designed to represent the geological, fluid, and operating conditions represented by Block X in the L Oilfield. Each fitted coefficient has a defined mathematical role in describing the pressure or temperature dependence of sand production, and the coupled formulation permits both variables to change simultaneously. Within the study block, the model may therefore serve as an engineering screening tool for comparing sand-production risk under different thermal-recovery schemes and for identifying combinations that warrant more detailed simulation or laboratory testing. Its fitting and preliminary verification remain specific to the geological setting, fluid properties, and operating ranges represented by the experiments. Application outside these ranges or to other reservoirs requires additional calibration and independent validation.

Table 7: Values of coefficients A, B, and C at different pressures.

Pressure (MPa)	Coefficient A	Coefficient B	Coefficient C
6	451.039	−503.178	−0.0049
8	389.888	−408.529	−0.0059
9	344.714	−346.040	−0.0072
10	324.822	−300.512	−0.0083
12	278.837	−279.389	−0.0206

Table 8: Values of coefficients D, E, and F at different temperatures.

Temperature (°C)	Coefficient D	Coefficient E	Coefficient F
80	73.991	10.059	0.225
105	123.739	7.245	0.237
120	151.784	4.789	0.254
130	168.440	3.776	0.265
155	207.237	2.168	0.277

Existing sand-production models have been developed primarily for cold production or conventional reservoir conditions and commonly require *in situ* stress, rock cohesion, internal friction angle, and other geomechanical inputs. The proposed model, by contrast, was developed from multicomponent thermal-fluid huff-and-puff experiments and explicitly incorporates the thermal-recovery variables of temperature and pressure. Because the models differ fundamentally in assumptions, inputs, and applicable operating conditions, a direct numerical comparison using the present experimental dataset is not feasible. Table 9 therefore compares their theoretical bases, controlling factors, and engineering applications, thereby clarifying the intended applicability of the proposed model under multicomponent thermal-fluid injection.

Table 9: Comparison of sand-production prediction models.

Comparison Item	Critical Pressure Difference Model	Mohr–Coulomb Model	Single-Factor Empirical Model	Model Proposed in This Paper
Theoretical Basis	Critical pressure difference theory	Rock strength criterion	Single-factor empirical fitting	Temperature-pressure coupled model
Main Controlling Factors	Pressure drawdown	*In situ* stress and rock strength	Temperature or pressure	Temperature and pressure
Engineering Applicability	Cold production reservoirs	Conventional reservoirs	Specific working conditions	Reservoirs undergoing multicomponent thermal-fluid huff-and-puff

To evaluate engineering applicability, the coupled pressure–temperature sand-production model was embedded in the multicomponent thermal-fluid huff-and-puff reservoir simulator for Block X in the L Oilfield and used to simulate the dynamic evolution of sand production. During simulation, sand-production intensity was recalculated from the local temperature and pressure fields in each grid block rather than assigned from fixed geomechanical parameters or a constant coefficient. This procedure enables dynamic prediction of the spatial and temporal evolution of reservoir sand production throughout thermal recovery.

The numerical model used a three-dimensional Cartesian grid of 40 × 40 × 20 cells (32,000 grid blocks). Grid spacing was 5 m in the X and Y directions and 1 m in the Z direction, covering the reservoir interval from 1200 to 1220 m. Reservoir properties were assigned from field data from Block X in the L Oilfield, including a porosity of 0.44, horizontal permeability of 3050 mD, vertical permeability of 305 mD, and a multicomponent thermal-fluid injection volume of 100 m^3 per cycle. Two representative injection scenarios were considered: (a) a low-temperature, low-pressure case (6 MPa, 120°C, CO_2/N_2 = 0.33) and (b) a high-temperature, high-pressure case (10 MPa, 190°C, CO_2/N_2 = 0.50). The spatial and temporal evolution of sand production under the two scenarios was then analyzed and compared.

As shown in Fig. 7, the sand-producing zone remained relatively limited under the low-temperature, low-pressure condition, with cumulative sand production of approximately 4.6 m^3 after 180 days. As temperature and pressure increased, thermal weakening intensified and the strength of the rock framework declined. Under the high-temperature, high-pressure condition, the sand-producing zone expanded, and cumulative sand production increased to 9 m^3 after 180 days.

Fig. 8 further compares the cumulative sand-production trajectories under the two conditions. The simulated trend is reported to be consistent with field observations that higher temperature and pressure aggravate reservoir sand production. During huff-and-puff production, the cumulative sand volume from a single well over 180 days is reported to range generally from 4 to 12 m^3. Under high-temperature, high-pressure, multicycle conditions, single-well cumulative sand production can exceed 10 m^3 and may be accompanied by extensive wormhole propagation and substantial deterioration of the rock framework.

The simulation results indicate that the coupled pressure–temperature model can reproduce the expected dynamic trend of sand production during multicomponent thermal-fluid huff-and-puff.

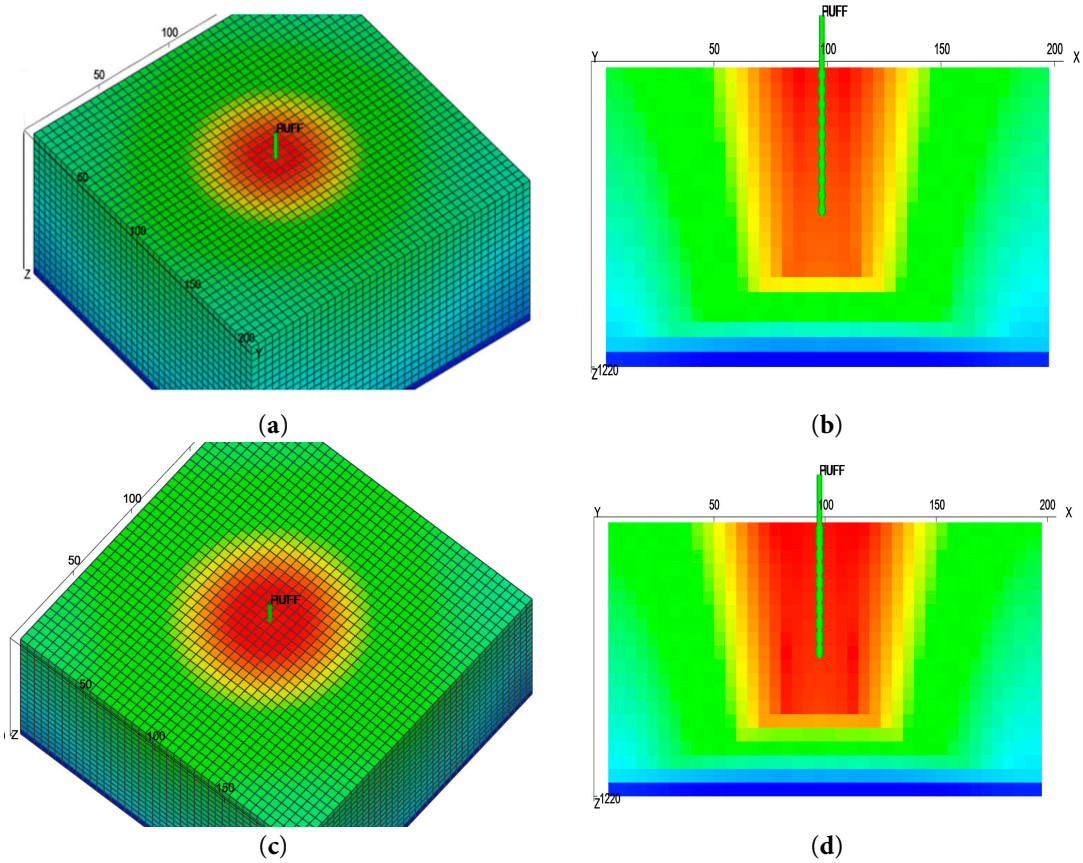

Figure 7: Simulated reservoir sand production after multicomponent thermal-fluid huff-and-puff. (**a**) Plan view under condition a; (**b**) cross-section under condition a; (**c**) plan view under condition b; and (**d**) cross-section under condition b.

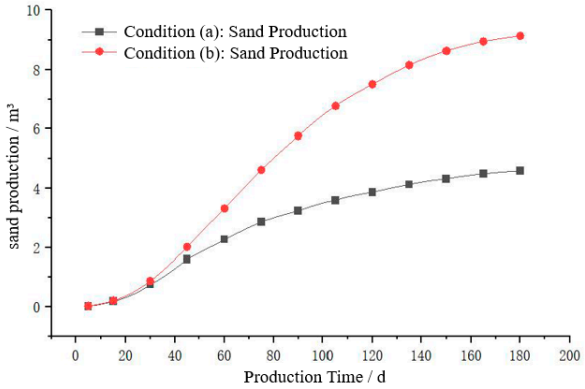

Figure 8: Comparison of simulated cumulative sand production under conditions a and b.

4 Conclusions

This study investigated an unconsolidated sandstone heavy-oil reservoir from Block X in the L Oilfield. Orthogonal sand-production experiments under multicomponent thermal-fluid and steam huff-and-puff conditions were used to compare rock mechanical properties and sand-production characteristics. The dominant factors, production mechanisms, and selected operating parameters were analyzed, and a coupled pressure–temperature sand-production model was developed. The main conclusions are as follows:

(1) Temperature and pressure were the statistically significant factors affecting both rock elastic modulus and produced-sand mass. Elastic modulus decreased, whereas sand production increased, as temperature and pressure rose. For elastic modulus, the F-value ranking was temperature > pressure > CO_2/N_2 volume ratio > injection volume for multicomponent thermal-fluid huff-and-puff and temperature > pressure > injection volume for steam huff-and-puff. For sand production, the ranking was pressure > temperature > injection volume > CO_2/N_2 volume ratio for multicomponent thermal-fluid huff-and-puff and temperature > pressure > injection volume for steam huff-and-puff.

(2) Multicomponent thermal-fluid stimulation weakened the rock framework more strongly and produced more sand than steam huff-and-puff because of CO_2 dissolution and N_2 gas channeling. The median particle size of the produced sand was approximately 200 μm, about twice that observed under steam stimulation. Large wormholes formed after the third multicomponent thermal-fluid cycle, whereas only smaller wormholes appeared after the fifth steam cycle.

(3) The selected operating parameters for multicomponent thermal-fluid huff-and-puff in the study block were 130°C, 10 MPa, a CO_2/N_2 volume ratio of 0.5, and an injection volume of 10 mL. This combination was intended to balance recovery performance against sand-production risk.

(4) The coefficient fits in the coupled pressure–temperature model had R^2 values of 0.94–0.99. The selected temperature-based formulation yielded a reported predicted–experimental correlation of 0.99, versus 0.98 for the alternative pressure-based formulation. The model quantitatively describes sand production within the tested multicomponent thermal-fluid conditions but requires independent validation before broader application.

Acknowledgement: This work was supported by the technical support and laboratory equipment support of each center.

Funding Statement: National Science and Technology Major Project “Study on key matching process technologies for heavy oil development with multi-component thermal fluid”.

Author Contributions: The authors confirm their contributions to the paper as follows: Research conception and design, initial draft preparation: Zhuwei Tao; results analysis: Shengda Zhang; Interpretation: Zetao Sun; data collection: Ying Wu; conception: Peng Li; resources: Xing Shi; review and editing: Hui Xu; supervision: Yanfeng He. All authors reviewed and approved the final version of the manuscript.

Availability of Data and Materials: The data that support the findings of this study are available from the corresponding author upon reasonable request.

Ethics Approval: Not applicable.

Conflicts of Interest: The authors declare no conflicts of interest.

References

1. Amin Y, Musa T, Ibrahim G, Elbashir N. Comprehensive evaluation of cyclic steam stimulation for enhanced heavy oil recovery: Assessing production and CO_2 emissions. J Petrol Explor Prod Technol. 2025;15(10):158. [CrossRef].
2. He C, Xu A, Fan Z, Zhao L, Cheng Y, Bo B, et al. Advanced mathematical model for reservoir heat efficiency with liquid in steam-injection wellbore. Energy Sources Part A Recovery Util Environ Eff. 2019;41(1):65–77. [CrossRef].
3. Song YW. Parameter optimization of multi-thermal fluid thermal recovery for Moertukete heavy oil reservoir. Inn Mong Petrochem Ind. 2023;49(7):60–3. (In Chinese).
4. Harding TG, Ali SMF, Flock DL. Steamflood performance in the presence of carbon dioxide and nitrogen. J Can Petrol Technol. 1983;22(5):9–17. [CrossRef].
5. Nasr TN, Prowse DR, Frauenfeld T. The use of flue gas with steam in bitumen recovery from oil sands. J Can Petrol Technol. 1987;26(3):43–9. [CrossRef].
6. Dong X, Liu H, Hou J, Zhang Z, John Chen Z. Multi-thermal fluid assisted gravity drainage process: A new improved-oil-recovery technique for thick heavy oil reservoir. J Petrol Sci Eng. 2015;133:1–11. [CrossRef].
7. Farahabadi ZT, Lashkarbolooki M. Effect of CO_2 on the interfacial tension and swelling of crude oil during carbonated water flooding. J Petrol Explor Prod Technol. 2023;13(1):353–64. [CrossRef].
8. Mahdavi S, Jalilian M, Dolati S. Review and perspectives on CO_2 induced asphaltene instability: Fundamentals and implications for phase behaviour, flow assurance, and formation damage in oil reservoirs. Fuel. 2024;368:131574. [CrossRef].
9. Perera MA, Ranjith PG, Rathnaweera TD, De Silva GD, Liu T. An experimental study to quantify sand production during oil recovery from unconsolidated quicksand formations. Petrol Explor Dev. 2017;44(5):860–5. [CrossRef].
10. Fetrati M, Pak A. Numerical simulation of sanding using a coupled hydro-mechanical sand erosion model. J Rock Mech Geotech Eng. 2020;12(4):811–20. [CrossRef].
11. Zhou ZY, Yu AB, Choi SK. Numerical simulation of the liquid-induced erosion in a weakly bonded sand assembly. Powder Technol. 2011;211(2–3):237–49. [CrossRef].
12. Rakhimzhanova A, Thornton C, Amanbek Y, Zhao Y. Numerical simulations of sand production in oil wells using the CFD-DEM-IBM approach. J Petrol Sci Eng. 2022;208:109529. [CrossRef].
13. Abbas AK, Baker HA, Flori RE, Al-hafadhi H, Al-haideri N. Practical approach for sand production prediction during production. In: Proceedings of the 53rd U.S. Rock Mechanics/Geomechanics Symposium; 2019 Jun 23–26; New York, NY, USA.
14. Alakbari FS, Mohyaldinn ME, Ayoub MA, Muhsan AS, Abdulkadir SJ, Hussein IA, et al. Prediction of critical total drawdown in sand production from gas wells: Machine learning approach. Can J Chem Eng. 2023;101(5):2493–509. [CrossRef].
15. Zhou B, Dong C, Song Y, Zhan X, Gwamba G, Bai H. Visualization-based experimental investigation of microscopic sand production characteristics and mechanisms in weakly consolidated sandstone reservoirs. Geoenergy Sci Eng. 2023;229:212054. [CrossRef].
16. Kozhagulova A, Shabdirova A, Minh NH, Zhao Y. An integrated laboratory experiment of realistic diagenesis, perforation and sand production using a large artificial sandstone specimen. J Rock Mech Geotech Eng. 2021;13(1):154–66. [CrossRef].
17. Song J, Li Y, Liu S, Xiong Y, Pang W, He Y, et al. Comparison of machine learning algorithms for sand production prediction: An example for a gas-hydrate-bearing sand case. Energies. 2022;15(18):6509. [CrossRef].
18. Shabdirova A, Hop Minh N, Zhao Y. Role of plastic zone porosity and permeability in sand production in weak sandstone reservoirs. Undergr Space. 2022;7(6):1003–20. [CrossRef].
19. Wang T, Chen S, Li M, An M. A resolved CFD-DEM investigation into sand production under water flooding in unconsolidated reservoir. Powder Technol. 2024;442:119859. [CrossRef].
20. Yu X, Liu X, Chen M, Wu G, Li X. Study on influence of heavy oil reservoir damage caused by multi-component thermal fluid huff and puff. Front Energy Res. 2022;10:821221. [CrossRef].

21. Guo M, Lun Z, Zhou B, Wang L, Liu H. Experimental study on water-rock interaction characteristics of unconsolidated sandstone during CO_2 multicomponent thermal fluid injection. Geofluids. 2023;2023:2197400. [CrossRef].
22. Mukherjee S, Gomez H. Effect of dissolved gas on the tensile strength of water. Phys Fluids. 2022;34(12):126112. [CrossRef].
23. Fu Q, Yang Z, Liu Y, Chen M. Research for flow behavior of heavy oil by N_2 foam-assisted steam (NFAS) flooding: Microscopic displacement experiment study. Processes. 2024;12(8):1775. [CrossRef].